Synthesis, characterization and magnetism of homoleptic bis(5-aryl-2-iminopyrrolyl) complexes of iron(II) and cobalt(II)

Tiago F. C. Cruz[a], Cláudia A. Figueira[a], João C. Waerenborgh[b], Laura C. J. Pereira[b], Yianling Li[c], Rodrigue Lescouëzec[c], Pedro T. Gomes[a,*]

[a] *Centro de Química Estrutural, Departamento de Engenharia Química, Instituto Superior Técnico, Universidade de Lisboa, Av. Rovisco Pais 1, 1049-001 Lisboa, Portugal.*

[b] *C²TN-Centro de Ciências e Tecnologias Nucleares, Instituto Superior Técnico, Universidade de Lisboa, 2695-066 Bobadela LRS, Portugal.*

[c] *Sorbonne Université, Institut Parisien de Chimie Moléculaire, IPCM, CNRS UMR 8232, 4 place Jussieu, 75252 Paris, France.*

* Corresponding author; Tel: +3518419612; E-mail: pedro.t.gomes@tecnico.ulisboa.pt

ABSTRACT: Four sterically congested and highly electronically unsaturated bis(5-aryl-2-iminopyrrolyl) ML_2 complexes of Fe(II) and Co(II), [M{κ²*N*,*N*-5-(2,6-R_2-C_6H_3)-NC_4H_2-2-C(H)=N(2,6-$^{i}Pr_2$-C_6H_3)}$_2$] (M = Fe, R = H (**1a**); M = Fe, R = Me (**1b**); M = Co, R = H (**2a**); M = Co, R = Me (**2b**)), were synthesized by metathetic reaction of the *in situ* prepared sodium salts of the new 5-aryl-2-(*N*-2,6-diisopropylformimino)pyrrole HL type ligand precursors (R = H (**Ia**), Me (**Ib**)) with $FeCl_2$ or $CoCl_2$, in moderate to good yields. The four-coordinate complexes were characterized by elemental analysis, X-ray diffraction, magnetic susceptibility measurements in solution and in solid state, and ^{57}Fe Mössbauer spectroscopy. All complexes have a high-spin electronic configuration, as measured both in solution, through the Evans method, and in solid state, through SQUID magnetic measurements, and Mössbauer spectroscopy for the case of Fe(II) complexes, displaying a tetracoordinated distorted tetrahedral coordination geometry about the respective metal center, as elucidated by X-ray diffraction. The inclusion of *ortho*-methyl groups in the 5-phenyl substituent of the 2-iminopyrrolyl ring in complexes **1b** and **2b** has an important influence in the structure of the complexes, giving rise to pronounced geometry distortions in particular for **1b.** This complex exhibits a see-saw-like geometry whereas a pyramidalization of the pyrrolyl nitrogen is observed for **2b**. Overall, the magnetic properties of the complexes can be rationalized by taking into account the effect of the magnetic anisotropy arising from the

second-order spin orbit coupling and the geometrical distortion. The simulation of the magnetic data using a zero-field splitting (ZFS) Hamiltonian led to values of the axial anisotropy, *D*, that are coherent for Co(II) and Fe(II) tetrahedral complexes, $D \approx -50$ cm^{-1} (**2a, 2b**) and 4 cm^{-1} (**1a**). In the case of **1b** the simulation evidenced a strong magnetic anisotropy with both axial and rhombic contributions ($D \approx -50$ cm^{-1}, $E \approx 10$ cm^{-1}) which are in line with the strongly distorted coordination sphere of the complex.

Keywords: 5-aryl-2-iminopyrrolyl ligands; four-coordinate complexes; Iron(II); Cobalt(II); structure and magnetic properties

1. Introduction

The chemistry of transition metals bearing bidentate ligands is of paramount importance in catalysis, for the most diverse transformations, as well as in materials science. In recent years, the use of earth-abundant metals instead of the platinum group elements has been a priority. Despite the clear economical advantage of earth-abundant metals, their low-coordinate heteroleptic chemistry with bidentate scaffolds remains relatively unexplored and somewhat unpredictable. For example, attempts to prepare low-valent or alkyl Fe and Co compounds of a single bidentate ligand led to disproportionation products of bis bidentate ligand metal compounds [1]. Despite the catalytic inactivity of these and other examples, homoleptic compounds of Fe and Co of bidentate ligands have still been attractive to other fields, such as magnetochemistry [2,3].

The chemistry of the bis bidentate 2-iminopyrrolyl framework has been modestly covered in the coordination chemistries of main-group elements, such as alkaline-earth metals (Mg, Ca, Sr, Ba) [4,5] or Al [4], of early transition metals (Zr [6], Ti [7], V [8] and Cr [9]) and of late transition metals (Ni [6,10–12], Cu [10,11] and Zn [4,13]). However, this simple scaffold is somehow reminiscent of porphyrins, which play a major role as ligands to biochemically relevant metals, such as Fe [14] and Co [15].

Specifically concerning the chemistry of Fe and Co bearing two 2-iminopyrrolyl bidentate ligands, to the best of our knowledge, only Bochmann *et al.* and our group have presented results with aryl substituents bonded to the iminic nitrogen atom. On one hand, Bochmann and co-workers reported bis bidentate bis(arylimino)pyrrolyl compounds of Fe(II) and Co(II), prepared from the 2,5-bis(arylimino)pyrrole ligand precursor HNC_4H_2-2,5-[CH=N(2,6-$^{i}Pr_2$-C_6H_3)]$_2$ [6]. On the other hand, we have also prepared and characterized a series of Co(II) unsaturated (15-electron) homoleptic complexes of the type [Co{2-(*N*-arylimino)pyrrolyl}$_2$], whereby tuning the steric bulkiness of the 2-aryliminopyrrolyl ligand, different coordination geometries of the Co(II) center were obtained, from tetrahedral (Chart 1, **A**) to the rarely observed square planar (Chart 1, **B**) [16]. In a different work, our group reported the unsuccessful attempts to prepare four-coordinate Fe(II) compounds of the type [Fe(2-(*N*-arylimino)pyrrolyl)$_2$], which were isostructural with **A**, ending up in uncharacterized products or in Fe(III) oxo complexes, the latter resulting from the oxidation of those highly reactive Fe(II) species with adventitious water molecules, owing to their unsaturated nature (14-electron species) [11]. In fact, the stabilization of those unsaturated species was achieved by

the simple addition of a donor ligand, such as pyridine, to the reaction medium, yielding the expected five-coordinate 16-electron Fe(II) complex (Chart 1, **C**) [11]. Similar pentacoordinated complexes of Co(II), containing the bis(2-formiminopyrrolyl) framework and a donor ligand, had been obtained with trimethylphosphine and tetrahydrofuran (Chart 1, **C**), but could only be prepared from the substitution reaction of the corresponding cobalt halide adducts ($[CoCl_2(PMe_3)_2]$ and $[CoCl_2(THF)_{1.5}]$) with 2 equivalents of the 2-iminopyrrolyl sodium salt, but not from the addition of PMe_3 or THF to complexes of the type **A** [17].

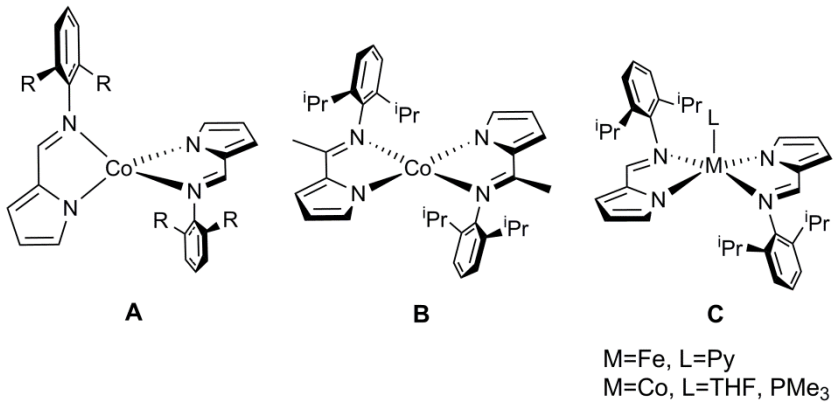


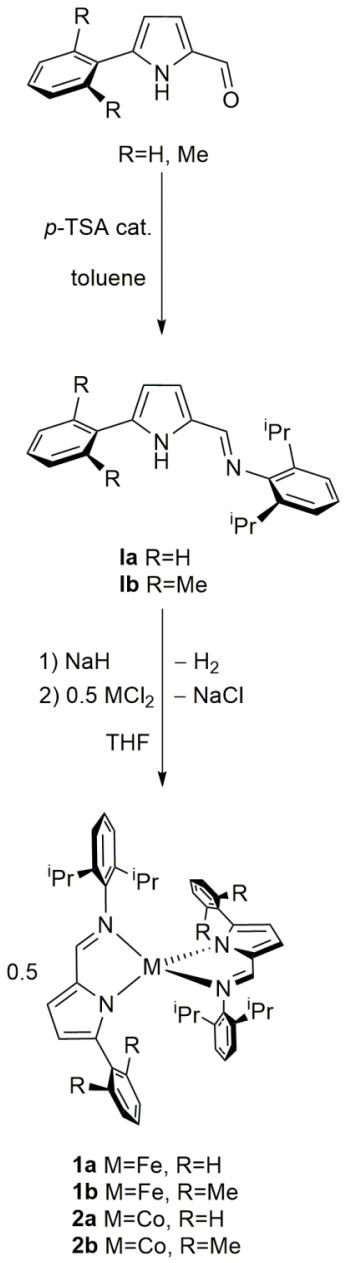
Chart 1

In the present work, we report the employment of sterically congested new 2-(*N*-arylformimino)pyrrole ligand precursors, which are substituted in position 5 of the pyrrole ring with phenyl rings (Scheme 1), in order to confer steric protection to the metal center and prepare stable highly unsaturated homoleptic Fe(II) bis(5-aryl-2-formiminopyrrolyl) complexes. We also describe the synthesis of the related homoleptic Co(II) bis(5-aryl-2-formiminopyrrolyl) complexes in order to compare their structure and properties with the previously reported analogous unsubstituted Co(II) bis(2-formiminopyrrolyl) complexes.[16] Both types of compounds are characterized by elemental analysis, single crystal X-ray diffraction, magnetic measurements in solution and in the solid state and ^{57}Fe Mössbauer spectroscopy.

2. Results and discussion

2.1. Syntheses of the ligand precursors and complexes

The new 5-aryl-2-(*N*-2,6-diisopropylformimino)pyrrole HL type ligand precursors used in this work were prepared in good yields (*ca.* 70-90%) from the catalytic condensation reaction of the previously reported 5-aryl-2-formyl-1*H*-pyrroles [18] with 2,6-diisopropyl aniline, in refluxing toluene (Scheme 1).



Scheme 1 Synthesis of the new 5-aryl-2-(*N*-2,6-diisopropylformimino)pyrrole ligand precursors and their corresponding Fe and Co complexes.

The corresponding homoleptic ML_2 complexes were synthetized in moderate to good yields by the salt metathesis of MCl_2, where M is Fe or Co, with two equivalents of the sodium salt of the respective ligand precursor (**Ia** or **Ib**) prepared *in situ* in a THF solution. After a standard work-up procedure, a *n*-hexane solution cooled to -20 ºC yielded orange-red crystals of the Fe(II) complexes **1a** and **1b**. The Co(II) complexes were obtained in a similar procedure, yielding dark red-green and dark red-brown crystals, respectively for **2a** and **2b**. (Scheme 1). These complexes were characterized by elemental analysis, single crystal X-ray diffraction, ^{1}H NMR spectroscopy, magnetic susceptibility measurements in solution and in the solid state, and Mössbauer spectroscopy for the case of the Fe(II) compounds.

The four complexes are soluble in *n*-hexane and show no signs of decomposition after heating their toluene solutions to 100 ºC for 24 h, under dinitrogen. These compounds are relatively stable in the crystalline state but their respective solutions are sensitive to air and moisture.

All complexes are paramagnetic and the Fe and Co centers are quite unsaturated, formally having 14 and 15 valence electrons, respectively. Magnetic susceptibility measurements in toluene-d_8 solutions of the Fe complexes **1a** and **1b** led to solution magnetic moments of 5.9 and 5.6 μ_B, respectively, as determined by the Evans method. On the other hand, using the same method, the Co complexes **2a** and **2b** display solution magnetic moments of 4.8 and 5.0 μ_B, respectively. These observations are in accordance with high-spin configurations of d^6 Fe(II) centers (S = 2; μ_{eff} = 4.9 μ_B) and d^7 Co(II) centers (S = 3/2; μ_{eff} = 3.88 μ_B), with spin-orbit coupling [16,19,20].

The complexes show paramagnetically shifted ^{1}H NMR spectra, ranging from 120 to −60 ppm in the most extreme cases. A striking difference is observed in the ^{1}H NMR spectra of complexes **1a**-**2a** (R = H) and **1b**-**2b** (R = Me) (the ^{1}H NMR spectra of the complexes are presented in Figs. S1-S4 of the Supplementary data). Complexes **1a**-**2a** show a set of resonances corresponding to a single 5-aryl-2-iminopyrrolyl moiety, indicating a C_2 symmetry, explained by the free rotation of the pyrrolyl 5-substituted phenyl rings. On the other hand, complexes **1b**-**2b** show a much higher number of resonances than expected for two magnetically equivalent 5-aryl-2-iminopyrrolyl moieties, hence displaying a C_1 symmetry. This difference is attributed to the hindered rotation generated by steric repulsion of the *ortho*-methyl groups of the 5-phenyl substituent of the pyrrolyl ring.

There are also marked differences in the solid-state structures of complexes **1a**-**2a** and **1b**-**2b**, obtained by single crystal X-ray diffraction.

2.2. X-ray diffraction studies

All complexes were obtained as crystals suitable for X-ray diffraction from concentrated *n*-hexane solutions cooled to -20 ºC. Complexes **1a**-**2a** and **1b**-**2b** crystallized in the triclinic and monoclinic crystal systems, in the P-1 and $P2_1/c$ space groups, respectively. The structures obtained by X-ray diffraction are displayed in Fig. 1, and a selection of bond lengths, bond angles and τ_4 parameters (0 for square planar and 1 for tetrahedral pure geometries) [21] of the structures are shown in Table 1. The crystallographic data of the compounds is presented in Table S1 of the Supplementary data.

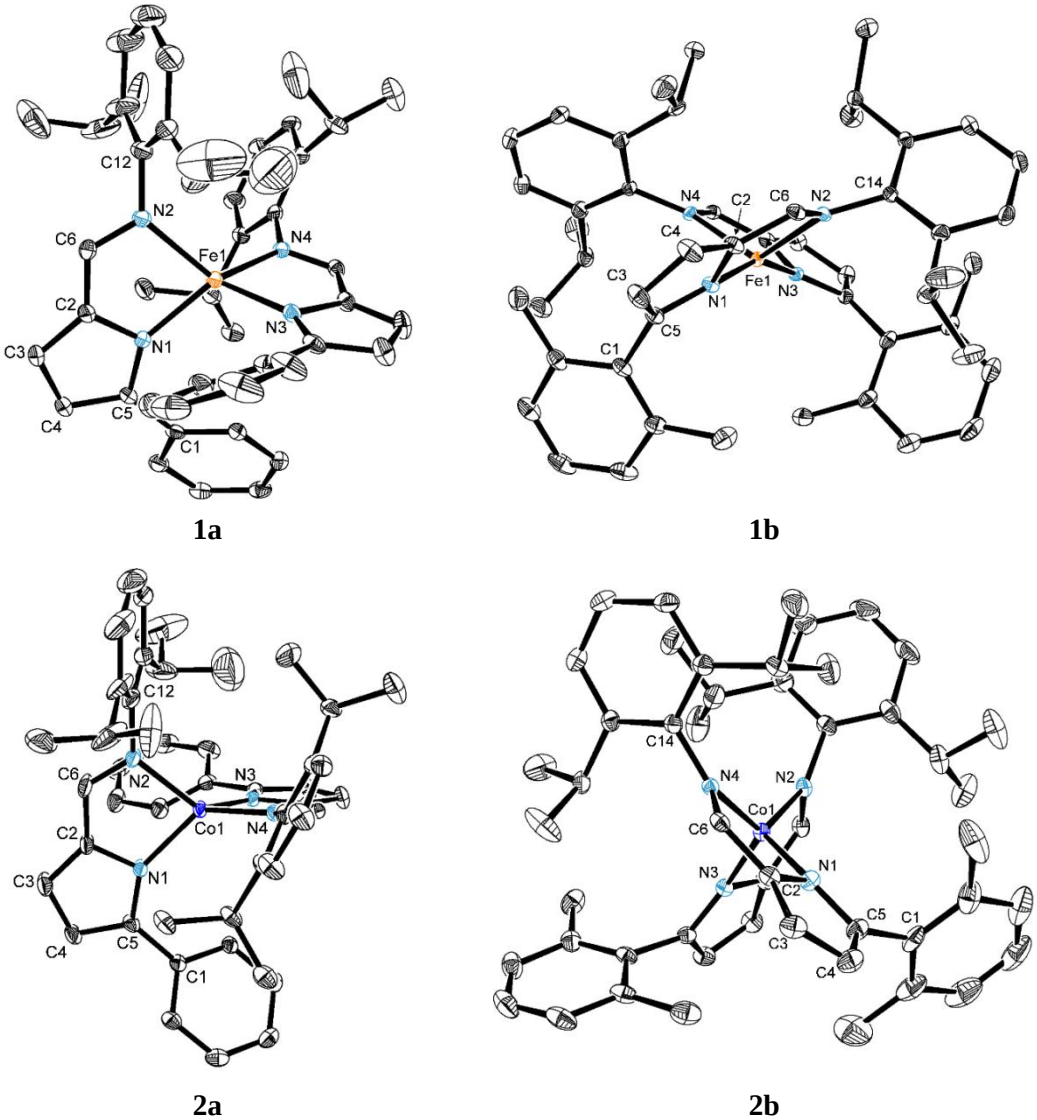


Fig. 1 ORTEP-3 diagrams of the X-ray diffraction structures of all four complexes, showing 30% probability ellipsoids. Hydrogen atoms are omitted for clarity.

Table 1 Selected bond distances (Å) and bond angles (º) for all complexes.

	1a	**1b**	**2a**	**2b**
Distances (Å)				
M1-N1	2.009(4)	2.0160(18)	1.976(3)	1.9899(18)
M1-N3	2.024(4)	2.0157(18)	1.983(3)	1.9990(18)
M1-N2	2.065(4)	2.1505(19)	2.037(3)	2.0306(17)
M1-N4	2.062(4)	2.1456(18)	2.039(4)	2.0392(18)
N1-C5	1.359(6)	1.364(3)	1.355(5)	1.351(3)
N1-C2	1.389(6)	1.385(3)	1.384(5)	1.386(3)
N2-C6	1.301(6)	1.303(3)	1.302(5)	1.307(3)
N2-C_{ipso}	1.430(6)	1.442(3)	1.433(5)	1.435(3)
C1-C5	1.475(7)	1.481(3)	1.474(6)	1.489(3)
C2-C3	1.392(7)	1.396(3)	1.389(6)	1.400(3)
C2-C6	1.405(7)	1.411(3)	1.407(6)	1.408(3)
C3-C4	1.388(7)	1.388(4)	1.391(6)	1.388(4)
C4-C5	1.395(7)	1.399(3)	1.395(6)	1.402(3)
Angles (º)				
N1-M1-N3	118.22(16)	155.74(7)	119.02(14)	114.90(7)
N1-M1-N2	83.38(16)	82.51(7)	83.83(13)	84.15(7)
N3-M1-N2	127.49(16)	105.97(7)	127.12(14)	126.23(7)
N1-M1-N4	130.15(19)	111.60(7)	128.66(17)	125.01(7)
N3-M1-N4	83.23(16)	82.06(7)	83.91(14)	85.11(7)
N2-M1-N4	120.37(16)	126.43(7)	120.00(14)	125.95(7)
C5-N1-C2	106.2(4)	106.60(19)	107.0(3)	106.68(18)
C6-N2-C_{ipso}	120.0(4)	118.7(2)	119.2(3)	119.22(17)
N1-C2-C3	109.9(4)	109.8(2)	109.7(4)	109.76(19)
N1-C2-C6	117.5(4)	119.0(2)	117.6(4)	116.89(18)
C3-C2-C6	132.4(4)	131.2(2)	132.5(4)	133.0(2)
C2-C3-C4	106.4(5)	106.4(2)	106.2(4)	106.2(2)
C3-C4-C5	107.4(5)	107.6(2)	107.7(4)	107.4(2)
N1-C5-C4	110.1(4)	109.6(2)	109.4(4)	110.0(2)
N1-C5-C1	121.8(5)	123.0(2)	122.6(4)	122.1(2)
C4-C5-C1	128.2(5)	127.2(2)	127.9(4)	127.1(2)
N2-C6-C2	120.5(4)	120.7(2)	119.0(3)	119.96(19)
τ_4	0.73	0.55	0.74	0.76

Complexes **1a**-**2a** are tetracoordinated entities, where two 5-phenyl-2-iminopyrrolyl ligands are coordinated to the metal center in a bidentate mode through the iminic (N2 and N4) and pyrrolyl (N1 and N3) nitrogen atoms in distorted tetrahedral geometries. The chelate bite angles in these complexes *i.e.* the N1−M−N2 are very similar in both structures (83.33(13)−83.38(16)º). On the other hand, the N1−M−N3 and N2−M−N4 angles are 118.22(16)−119.02(14)º and 120.00(14)−120.37(16)º, respectively for complexes **1a** and **2a**, pointing to a distorted tetrahedral geometry (τ_4=0.73−0.74). The M−N1 and M−N2 bond lengths are also close: 2.009(4)−2.065(4) Å in the Fe complex **1a** and 1.976(3)−2.039(4) Å in the Co complex **2a**. The angles between the planes corresponding to the five membered chelates are 81.1 and 82.2º for **1a** and **2a**, respectively. These observations are in accordance with the structural data of homoleptic bis(2-iminopyrrolyl) Co(II) compounds reported previously by our group, which were unsubstituted in position 5 of the pyrrolyl ring [16]. The torsions of the 2,6-diisopropylphenyl ring (bonded to the iminic nitrogen) relative to the 2-iminopyrrolyl moieties are in the range of 64.54−74.08º, which are lower than the values previously observed [16]. This may be attributed to the steric repulsion generated by the 5-phenyl substitution. On a related observation, the torsions of the 5-phenyl ring relative to the 2-iminopyrrolyl moiety are in the range of 31.35−31.98º.

The coordination geometry of complex **2b** is very similar to those of complexes **1a**-**2a**, with the Co-N bond lengths and the N−Co−N bond angles falling in the same range, giving rise to a similar τ_4 parameter (0.76). Also, the angle between the planes defined by N1−Co1−N2 and N3−Co1−N4 is 84.68º, which is comparable to those of complexes **1a**-**2a**. The torsions of the 2,6-diisopropylphenyl ring bonded to the iminic nitrogen and of the 5-(2,6-dimethylphenyl) ring relative to the 2-iminopyrrolyl moiety are in the range of 75.39−79.36º and 77.27−82.08º, respectively. Furthermore, the five-membered chelates (defined by the atoms Co1−N1−C2−C6−N2 and Co1−N3−C25−C29−N4) are significantly deviated from planarity (19.2−22.7º), with a clear pyramidalization of the pyrrolyl nitrogen atoms, as opposed to the near planar chelates in complexes **1a**-**2a**. These last observations for complex **2b** are attributed to the extra stereochemical stress imparted by the 2,6-dimethylphenyl substituents.

Complex **1b** is also tetracoordinated, the ligands exhibiting the typical bidentate coordination mode. The Fe−N bond lengths are in the expected range and the chelate bite angles are also very similar to those of complexes **1a**, **2a** and **2b**. Contrasting with these similarities, the main difference stands in the N−Fe−N bond angles between the two ligands, giving rise to a τ_4 parameter of 0.55, an intermediate case between tetrahedral and square

planar [21]. The angle between the planes defined by N1−Fe1−N2 and N3−Fe1−N4 is 63.37(7)º, being much more deviated from orthogonality than in the remaining complexes. As in complex **2b**, albeit not as pronounced, the five-membered chelation rings in complex **1b** are also modestly deviated from planarity (10.2−16.0º), with the pyrrolyl nitrogen atom in a slight pyramidal conformation. The marked differences between complexes **1b** and **2b** are explained by the additional steric bulkiness of the 2,6-dimethylphenyl groups: (a) planar chelation rings of the respective ligands in complex **1b** but a very distorted coordination geometry; (b) pyramidalized pyrrolyl nitrogen atoms in complex **2b**, but a less distorted coordination geometry.

The resulting highly distorted geometry of complex **1b** can be better described as: (a) a seesaw-like geometry, in which the quite linear N1–Fe1–N3 (155.74(7)º) forms the plank and the N2–Fe1–N4 (126.43(7)º) forms the pivot, similar to that observed by Bochmann *et al.* in the only crystalographically characterized Fe(II) compound supported by the bis(2-iminopyrrolyl) scaffold [6]; or (b) a severely distorted trigonal pyramidal geometry (τ_4= 0.85 in the pure undistorted case [21]), in which N1, N3 and N4 form the trigonal plane with the Fe1 atom sitting only 0.309 Å above it and N2 occupying the distorted apical position, with the Fe1-N2 bond forming an angle of 82.51º with that plane, the best example in the literature of a Fe trigonal pyramidal geometry being that of Fe(II) complexes supported by tris(pyrrolyl-α-methyl)amine tripodal ligands reported by Chang *et al*. [3] Alternatively, the geometry of **1b** could also be regarded as reminiscent of distorted trigonal bipyramidal, in which N1 and N3 are in the apical positions, N2 and N4 occupy two equatorial positions, the remaining third equatorial position being vacant. This vacant position makes complex **1b** more susceptible of additional reactivity (namely towards water and oxygen) since its Fe atom is more coordinatively exposed than in compounds **1a**, **2a** and **2b**, as shown in their spacefill views (Fig. S5 of the Supplementary data).

2.3. Magnetic susceptibility measurements in the solid state

In order to confirm the electronic states of the complexes and understand how these geometrical distortions could affect the magnetic properties of these complexes, measurements in the solid state of the four complexes of Fe (**1a** and **1b**) and Co (**2a** and **2b**) were carried out. The magnetic susceptibility was thus measured as a function of temperature in the range of 5-300 K. The plots of the $\chi_M T$ *vs. T* measured at 500 Oe are shown in Fig. 2

(χ_M is the molar magnetic susceptibility per formula unit). These measurements revealed a paramagnetic character for these complexes. At room temperature, the $\chi_M T$ product of the Fe complexes **1a** and **1b** was found to be 3.94 and 3.91 cm^3 mol^{-1} K, respectively. These values are higher than the spin-only value expected for tetrahedral Fe(II) complexes with an isotropic $^5A_1$ electronic ground state ($\chi_M T$ = 3.0 cm^3 mol^{-1} K for S = 2 and g = 2). They result from an efficient mixing of the ground state with (orbitally unquenched) excited states, as it was previously observed in other tetrahedral Fe(II) complexes [20,22]. These results are coherent with the magnetic susceptibility measurements performed in solution using the Evans method mentioned above (see also Table 2, μ_{eff} = 2.84 $(\chi_M T)^{1/2}$) and the electronic configuration agree with the ^{57}Fe Mössbauer data referred below.

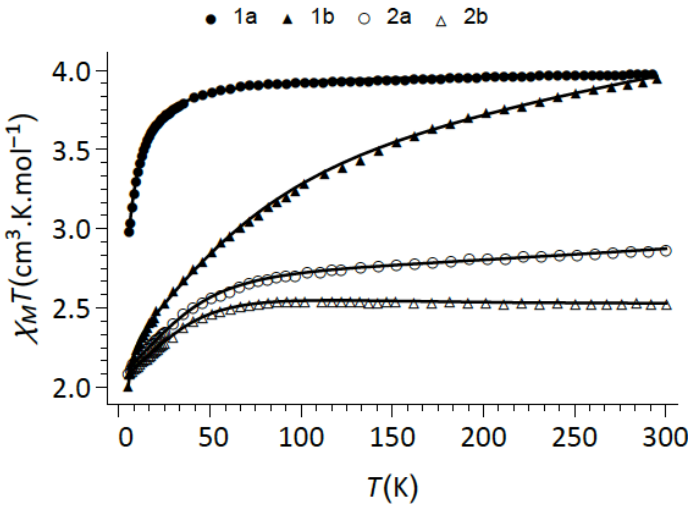


Fig. 2 Temperature dependence of the product of molar magnetic susceptibility with temperature, $\chi_M T$, with a magnetic field of 500 Oe for Fe (**1a**, **1b**; full symbols) and Co (**2a**, **2b**; open symbols) complexes. The lines represent the best simulation (see text).

Table 2 Effective magnetic moments μ_{eff} (μ_B) for the Fe(II) (**1a**, **1b**) and Co(II) (**2a**, **2b**) complexes, measured in toluene-d_8 solution (Evans method) and in the solid state (SQUID method), at r.t.

Complex	Evans	SQUID
	μ_{eff} (μ_B)	μ_{eff} (μ_B)
1a	5.9	5.64
1b	5.6	5.62
2a	4.8	4.79
2b	5.0	4.50

Although presenting a similar value at room temperature (r.t.), the $\chi_M T$ *vs* T curves of the complexes **1a** and **1b** behave differently. With the decrease of temperature, complex **1a** is

almost temperature independent down to 35 K. Below 35 K it decreases until reaching the value of 2.95 cm^3 mol^{-1} K, at 5 K. For complex **1b**, from room temperature down to 5 K, a continuous decrease of the $\chi_M T$ product is observed, reaching at 5 K the value 1.98 cm^3 mol^{-1} K, lower than that of **1a**. Since the interatomic distances between Fe-Fe atoms are very large in both cases (> 10 Å), the non-Curie behaviour cannot be ascribed to intermolecular magnetic interactions. They are rather due to the magnetic anisotropy of the complexes, which can result from the second order spin-orbit coupling and some geometrical distortion in the coordination sphere [23]. A larger distortion in **1b** could lead to a stronger anisotropy. In order to quantify this effect, the magnetic properties were simulated with the PHI program [24] and by using the following Hamiltonian:

$$\widehat{H} = D\hat{S}_z^{\,2} + E(\hat{S}_y - \hat{S}_x) + g\mu_B \boldsymbol{SH}$$

The first term is the zero-field splitting (ZFS), an effective spin Hamiltonian, which accounts for the magnetic anisotropy. *D* and *E* are the axial and rhombic anisotropy terms, respectively. μ_B is the Bohr magneton and *g* is the Landé factor. In our simulations, we had to consider an axial *g* tensor to obtain satisfactory results. The best fit for **1a** was obtained for: *D* = 4.8 cm^{-1} and $g_1 = g_2 = 2.12$, $g_3 = 2.63$. These values are coherent with those found in previously reported tetrahedral Fe(II) complexes [22]. The simulation of **1b** led to a strongly negative D value and it was necessary to take into account the transverse anisotropy, *E* The best fit was obtained with the following set of parameters: *D* = -53.8 cm^{-1}, *E* = 9.2 cm^{-1}, $g_1 = g_2 = 2.18$, $g_3 = 2.13$ (positive values of *D* lead to unreasonable values of *g*). The higher anisotropy observed in **1b** is very likely due to the peculiar distortion of its coordination sphere. Most of the Fe(II) tetrahedral complexes previously reported exhibit a similar behaviour as **1a**, however it is worth noticing that such large D values have been predicted by E. Ruiz *et al.* in distorted tetrahedral complexes [25].

The $\chi_M T$ values measured at room temperature for the Co complexes **2a** and **2b** are 2.84 and 2.51 cm^3 mol^{-1} K (Fig. 2), respectively. They agree well with the magnetic moments determined by the Evans method (Table 2) suggesting that the structures of the complexes are similar in solution and in the solid state. The experimental values are significantly above the calculated spin-only value for high-spin Co(II), 1.86 cm^3 mol^{-1} K (*S* = 3/2 and *g* = 2), but well within the range of the observed experimental values for Co(II) compounds [16,19,20]. Upon cooling, the $\chi_M T$ values remain almost constant down to *ca.* 100 K and then decrease

continuously reaching the value of 2.07 cm^3 mol^{-1} K at 5 K. As for the Fe complexes, the long distances between the complexes in the crystal lattice allow discarding the influence of intermolecular exchange interactions. This behaviour is thus ascribed to the effect of the second order spin-orbit coupling that leads to a magnetic anisotropy. The magnetic data were thus simulated following the same procedure as the one described above. The best simulations were obtained for the following set of parameters: D = -53.0 cm^{-1}, $g_1 = g_2$ = 2.10, g_3 = 2.70, for **2a**, and D = -51.3 cm^{-1}, $g_1 = g_2$ = 2.01, g_3 = 2.69, for **2b**. The values obtained for these parameters in both complexes are very close, which is coherent with the structural similarities between them. They are also similar to those obtained in the literature for similar tetracoordinated Co(II) complexes.[2,26].

2.4. Mössbauer spectroscopy

The Mössbauer spectra of **1a** (Fig. 4) show a single quadrupole doublet with estimated isomer shift relative to metallic αFe at 295 K, IS, and quadrupole splitting, QS (Table S2 of the Supplementary data) consistent with high-spin Fe(II), S = 2, in a distorted tetrahedral coordination [27]. In the measured temperature range, 295–1.7 K, the samples are paramagnetic and the spectra evidence no magnetic transition.

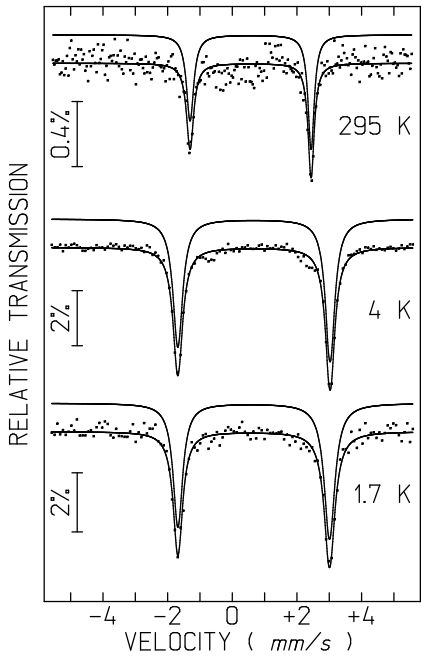


Fig. 3 Mössbauer spectra of complex **1a** taken at different temperatures. The line on the experimental points is the calculated doublet due to Fe(II) in the S = 2 spin state.

The spectra of complex **1b** (Fig. 5) in the temperature range 70–295 K show, in addition to high-spin Fe(II), a second doublet with lower IS and QS consistent with high-spin Fe(III) [27]. This assignment is confirmed by the 4 K measurement where the small QS doublet gives rise to a sextet with magnetic hyperfine field (Table S2 of the Supplementary data) typical for high-spin, S = 5/2, Fe(III). No magnetic transition is observed for Fe(II) in the range 4–295 K. The observed increase in the IS values, for both samples **1a** and **1b**, as the temperature decreases from 295 K down to 4 K is explained by the second order Doppler shift [27]. The presence of Fe(III) in sample **1b** in the Mössbauer absorber is consistent with the fact that this complex is considerably more unstable than **1a**, since in both cases the perspex sample holder, which was filled with the sample in a glovebox, is not airtight and was handled in air in its transfer to the spectrometer. At variance, as referred above, the sample **1b** used for the SQUID experiments was transferred to a quartz tube in a glovebox and sealed under dinitrogen. Consequently, the sample **1b** used for SQUID measurements was not oxidized.

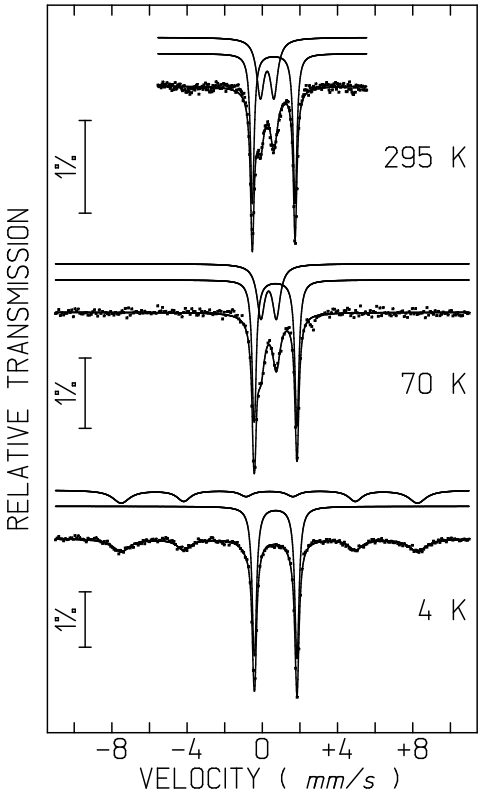


Fig. 4 Mössbauer spectra of complex **1b** taken at different temperatures. The line on the experimental points is the sum of the calculated doublet due to Fe(II) in the S = 2 spin state and the doublet (295 and 70 K) or sextet (4 K) due to Fe(III) in the S = 5/2 spin state.

The estimated QS values for Fe(II) in **1a** and **1b** (Table S2 of the Supplementary data) confirm that the coordination geometry distortion of the Fe(II) site in **1b** is very high, in particular much stronger than in **1a**. High-spin Fe(II) quadrupole splittings depend both on the electric field gradient arising from the lattice charge distribution, q_{latt}, and on due to the *d* electron distribution [28]. The *d* electron distribution depends on the crystal field and on the occupation of the ground and first excited states. Parameters q_{latt} and q_{el} have opposite signs and the absolute value of q_{el} is higher than q_{latt} since the electronic charge distribution is much closer to the Fe nuclei than the charges of the lattice. The total quadrupole splitting is therefore directly related to q_{el} - q_{latt}. If there are no phase transitions between 4 K and 295 K, q_{latt} remains approximately constant in the same temperature range. On the other hand, if there are low-lying excited electronic states, q_{el} decreases with increasing temperature as observed for **1a**. However, if the coordination geometry distortion is huge, the occupation of electronic excited states is negligible in the 4–295 K temperature range and, in this case, QS of high-spin Fe(II) will be temperature independent, as observed for **1b**. Furthermore, QS for the more distorted site in **1b** is expected to be lower than in **1a** since q_{latt} for **1a** is much lower than for **1b** and therefore q_{el} - q_{latt} will be higher for the least distorted site.

3. Conclusions

A family of highly electronically unsaturated Fe(II) and Co(II) bis(5-aryl-2-iminopyrrolyl) complexes of the type [M{κ^2*N*,*N*-5-(2,6-R_2-C_6H_3)-NC_4H_2-2-C(H)=N(2,6-$^i Pr_2$-C_6H_3)}$_2$], with M=Fe (**1**) or Co (**2**) and R=H (**a**) or Me (**b**), has been prepared and characterized. The two sterically congested new 5-aryl-2-iminopyrrolyl ligands protect the metal center giving rise to isolable homoleptic four-coordinate complexes with distorted tetrahedral geometries, as indicated by X-ray diffraction studies. Magnetic measurements in solution and in the solid state, as well as ^{57}Fe Mössbauer spectroscopy demonstrated high-spin states for all four complexes.

The distortion of the Fe(II) site on **1b** is particularly strong as evidenced not only by the X-ray diffraction studies but also by the temperature independent value of the Fe(II) quadrupole splitting in Mössbauer data. This strong distortion leads to a more coordinatively exposition of the Fe atoms than in compounds **1a**, **2a** and **2b**, and consequently to a higher sensitivity to air and moisture of **1b**. The solid-state magnetic study is coherent with the structural data and the simulation of the $\chi_M T$ *vs* *T* curve of **1b** revealed a high magnetic

anisotropy with both axial and rhombic ZFS contributions, which is quite uncommon for tetracoordinated Fe(II) complexes.

4. Experimental

4.1. General

All operations were performed under dry dinitrogen atmosphere using standard glovebox and Schlenk techniques. Solvents were pre-dried with molecular sieves and distilled by refluxing under dinitrogen for several hours over suitable drying agents (sodium/benzophenone for THF; CaH_2 for *n*-hexane). Solvents and solutions were transferred using a positive pressure of nitrogen through stainless steel cannulae and mixtures were filtered in a similar way using modified cannulae that could be fitted with glass fiber filter disks.

The compounds 5-phenyl-2-formyl-1*H*-pyrrole and 5-(2,6-dimethylphenyl)-2-formyl-1*H*-pyrrole were prepared as reported in the literature [18].

Elemental analyses were obtained from the IST elemental analysis services.

4.2. Synthesis of the ligand precursors

*4.2.1. 5-phenyl-2-(N-2,6-diisopropylphenylformimino)pyrrole (**Ia**)*

5-phenyl-2-formyl-1*H*-pyrrole (0.748 g; 4.4 mmol), 2,6-diisopropylaniline (0.80 ml; 4.2 mmol) and a catalytic amount of *p*-toluenesulfonic acid (0.040 g; 0.21 mmol) were suspended in toluene (20 ml) in a round-bottom flask and the mixture refluxed at 140 ºC for 60 hours. After cooling to room temperature the solvent was removed under vacuum. Extraction with *n*-hexane gave a brown-orange solution, in which the product and aniline reagent co-precipitated together. The *n*-hexane was evaporated and the residue dried in high vacuum, at 120 ºC, in order to evaporate the excess of reagent. The remaining oily paste was re-dissolved in *n*-hexane and stored at -20 ºC. The brown solid precipitate of **Ia** was filtered and dried under vacuum. Yield: 1.23 g (86%).

Anal. Calc. for $C_{23}H_{26}N_2 \cdot 0.25(\text{-}Si(CH_3)_2O\text{-})$: C, 80.87; H, 7.94; N, 8.03. Found: C, 80.23; H, 8.04; N, 8.13. ^{1}H NMR (300 MHz, $CDCl_3$): δ N*H* resonance absent, 7.93 (s, 1H, C*H*=N), 7.65 (d, $^3J_{HH}$ = 7.5 Hz, 2H, 5-Ph-H$_{ortho}$), 7.43 (t, $^3J_{HH}$ = 7.6 Hz, 2H, 5-Ph-H$_{meta}$), 7.31 (t, $^3J_{HH}$ = 7.3 Hz, 1H, 5-Ph-H$_{para}$), 7.19-7.12 (m, 3H, N-Ph-H$_{meta}$ and N-Ph-H$_{para}$), 6.69 (d, $^3J_{HH}$ = 3.6

Hz, 1H, H_3 *pyrr*), 6.64 (d, $^3J_{HH}$ = 3.7 Hz, 1H, H_4 *pyrr*), 3.13-2.99 (m, 2H, C*H*$(CH_3)_2$), 1.18 (d, $^3J_{HH}$ = 6.9 Hz, 12H, CH(C*H*$_3)_2$). $^{13}C\{^1H\}$ NMR (75 MHz, $CDCl_3$): δ 151.8 (*C*H=N), 148.7 (N-Ph-C_{ipso}), 138.5 (N-Ph-C_{ortho}), 136.7 (C_5 *pyrr*), 131.5 (5-Ph-C_{ipso}), 130.9 (C_2 *pyrr*), 129.0 (5-Ph-C_{meta}), 127.6 (5-Ph-C_{para}), 124.7 (5-Ph-C_{ortho}), 124.1 (N-Ph-C_{para}), 123.1 (N-Ph-C_{meta}), 117.6 (C_3 *pyrr*), 107.9 (C_4 *pyrr*), 27.9 (*C*H$(CH_3)_2$), 23.7(CH(*C*$H_3)_2$).

*4.2.2. 5-(2,6-dimethylphenyl)-2-(N-2,6-diisopropylphenylformimino)pyrrole (**Ib**)*

5-(2,6-dimethylphenyl)-2-formyl-1*H*-pyrrole[18] (0.636 g; 3.2 mmol), 2,6-diisopropylaniline (0.71 mL; 3.8 mmol) and a catalytic amount of *p*-toluenesulfonic acid (30 mg; 0.16 mmol) were suspended in toluene (20 ml) in a round-bottom flask and the mixture refluxed at 140 ºC for 48 hours. After cooling to room temperature the solvent was removed under vacuum. Purification was carried out by column chromatography with *n*-hexane:ethyl acetate (4:1) as eluent. The combined fractions were evaporated, yielding **Ib** as a dark orange solid. Yield: 0.870 g (76%).

Anal. Calc. for $C_{25}H_{30}N_2$·0.065(-Si$(CH_3)_2$O-): C, 83.06; H, 8.44; N, 7.71. Found: C, 82.92; H, 8.80; N, 7.74. ^1H NMR (300 MHz, $CDCl_3$): δ 9.15 (br, 1H, N*H*), 7.96 (s, 1H, C*H*=N), 7.24-7.21 (m, 1H, 5-Ph-H_{para}), 7.18-7.09 (m, 5H, 5-Ph-H_{meta}, N-Ph-H_{meta} and N-Ph-H_{para}), 6.71 (d, $^3J_{HH}$ = 3.3 Hz, 1H, H_3 *pyrr*), 6.23 (d, $^3J_{HH}$ = 3.3 Hz, 1H, H_4 *pyrr*), 3.14-3.00 (m, 2H, C*H*$(CH_3)_2$), 2.28 (s, 6H, C*H*$_3$), 1.20 (d, $^3J_{HH}$ = 6.9 Hz, 12H, CH(C*H*$_3)_2$). $^{13}C\{^1H\}$ NMR (75 MHz, $CDCl_3$): δ 151.5 (*C*H=N), 149.2 (N-Ph-C_{ipso}), 138.4 (N-Ph-C_{ortho}), 138.3 (5-Ph-C_{ortho}), 134.7 (C_5 *pyrr*), 132.6 (5-Ph-C_{ipso}), 130.3 (C_2 *pyrr*), 128.6 (5-Ph-C_{para}), 127.7 (5-Ph-C_{meta}), 124.0 (N-Ph-C_{para}), 123.2 (N-Ph-C_{meta}), 116.0 (C_3 *pyrr*), 110.8 (C_4 *pyrr*), 28.1 (*C*H$(CH_3)_2$), 23.7 (CH(*C*$H_3)_2$), 20.9 (*C*H_3).

4.3. Synthesis of the complexes

*4.3.1. General method for the synthesis of [M{κ^{2}N,N-5-(2,6-R_2-C_6H_3)-NC_4H_2-2-C(H)=N(2,6-^{i}Pr$_2$-C_6H_3)}$_2$] (M= Fe (**1**) or Co (**2**) and R= H (**a**) or Me (**b**))*

NaH (2.2 equivalents) was suspended in THF and **Ia** (R = H) or **Ib** (R = Me) (2 equivalents) was added as a solid, under a counter flow of dinitrogen, yielding a pale red suspension. The mixture was stirred for 3 h at 80 ºC under dinitrogen, yielding brown (for R = H) or pale orange (for R = Me) suspensions. The suspension was allowed to settle as it cooled to room temperature. This solution was filtered and added dropwise to a THF suspension of

anhydrous MCl_2 (M= Fe or Co; 1 equivalent), which was cooled to -78 ºC. The mixture was allowed to warm up to room temperature while stirring overnight. All volatile materials were evaporated under reduced pressure and the residue dried under vacuum. The solid was extracted with *n*-hexane until extracts were colorless. The extracts were combined and the resulting solution was concentrated and stored at -20 ºC. After a few days, the title compounds were obtained as crystalline solids suitable for X-ray diffraction.

*4.3.1.1. [Fe{κ^{2}N,N'-5-(C_6H_5)-NC_4H_2-2-C(H)=N(2,6-^{i}Pr_2-C_6H_3)}$_2$] (**1a**)*

This complex was prepared as described above, using $FeCl_2$ (0.064 g, 0.5 mmol), the ligand precursor **Ia** (0.33 g, 1 mmol) and NaH (0.026 g, 1.1 mmol) and obtained as a red crystalline solid. Yield: 0.14 g (39%).

Anal. Calc. for $C_{46}H_{50}FeN_4$: C, 77.30; H, 7.05; N, 7.84. Found: C, 76.31; H, 7.36; N, 7.76. μ_{eff} (toluene-d_8) = 5.9 μ_b. ^{1}H NMR (300 MHz, C_6D_6): δ 59.6, 54.9 (br) 24.0 (br), 20.1, 13.8, 9.6, 9.2 (br), 5.2 (br), 1.2, 0.9 (br), -1.0, -3.9 (br), -9.2, -27.2.

*4.3.1.2. [Fe{κ^{2}N,N'-5-(2,6-Me_2-C_6H_3)-NC_4H_2-2-C(H)=N(2,6-^{i}Pr_2-C_6H_3)}$_2$] (**1b**)*

This complex was prepared as described above, using $FeCl_2$ (0.064 g, 0.5 mmol), the ligand precursor **Ib** (0.36 g, 1 mmol) and NaH (0.026 g, 1.1 mmol) and obtained as a red crystalline solid. Yield: 0.20 g (52%).

Anal. Calc. for $C_{50}H_{58}FeN_4$: C, 77.59; H, 7.58; N, 7.27. Found: C, 76.88; H, 7.67; N, 7.21. μ_{eff} (toluene-d_8) = 5.6 μ_b. ^{1}H NMR (300 MHz, toluene-d_8): δ 67.6, 40.5 (br), 31.9, 21.6 (br), 18.5, 16.4, 10.1 (br), 7.4, 6.3, 1.9 (br), 0.9 (br), -2.8, -10.9 (br), -30.4 (br).

*4.3.1.3. [Co{κ^{2}N,N'-5-(C_6H_5)-NC_4H_2-2-C(H)=N(2,6-^{i}Pr_2-C_6H_3)}$_2$] (**2a**)*

This complex was prepared as described above, using $CoCl_2$ (0.097 g, 0.75 mmol), the ligand precursor **Ia** (0.49 g, 1.5 mmol) and NaH (0.038 g, 1.6 mmol) and obtained as a dark red-green crystalline solid. Yield: 0.350 g (67%).

Anal. Calc. for $C_{46}H_{50}CoN_4$: C, 76.96; H, 7.02; N, 7.80. Found: C, 76.59; H, 7.40; N, 7.84. μ_{eff} (toluene-d_8) = 4.8 μ_b. ^{1}H NMR (300 MHz, C_6D_6): δ 39.6 (br), 19.0 (br), 7.7 (br), 0.4 (br), -12.6, -17.0, -22.5 (br), -24.4 (br), -.27.2.

*4.3.1.4. [Co{κ²N,N'-5-(2,6-Me₂-C₆H₃)-NC₄H₂-2-C(H)=N(2,6-ⁱPr₂-C₆H₃)}₂] (**2b**)*

This complex was prepared as described above, using $CoCl_2$ (0.065 g, 0.5 mmol), the ligand precursor **Ib** (0.36 g, 1 mmol) and NaH (0.026 g, 1.1 mmol) and obtained as a dark red crystalline solid. Yield: 0.24 g (61%).

Anal. Calc. for $C_{50}H_{58}CoN_4$: C, 77.59; H, 7.55; N, 7.24. Found: C, 77.22; H, 7.66; N, 7.26. μ_{eff} (toluene-d_8) = 5.0 μ_b. ^{1}H NMR (300 MHz, C_6D_6): δ 112.1 (br), 101.7, 83.0 (br), 56.9, 37.9 (br), 28.4 (br), 16.1 (br), 14.5, 6.6, -2.0 (br), -3.0, -4.4, -6.4, -7.6, -8.4 (br), -8.9, -10.5, -12.6 (br), -14.2 (br), -19.3, -21.6 (br), -23.3, -25.2, -26.5 (br), -33.9 (br), -48.9 (br), -52.1 (br).

4.4. NMR measurements

The NMR spectra of the ligand precursors and complexes were recorded on a Bruker "AVANCE III" 300 MHz spectrometer at 299.995 MHz (^{1}H) and 75.4296 MHz (^{13}C) and referenced to the residual protio-resonances of the corresponding solvents (^{1}H) and to the carbon resonances of the solvents (^{13}C). The samples were prepared in a glovebox in normal (ligand precursors) and J. Young (complexes) NMR tubes. Deuterated solvents were dried over activated 4 Å molecular sieves and degassed by the freeze-pump-thaw technique.

The solution magnetic susceptibility measurements of compounds **1a,b** and **2a,b** were carried out by the Evans method [29], using a 3% solution of hexamethyldisiloxane (internal reference) in toluene-d_8. These solutions were prepared in a glovebox in J. Young NMR tubes containing capillary tubes filled with the same solvent mixture, in which the hexamethyldisiloxane is the external reference.

4.5. X-ray diffraction

Crystallographic and experimental details of crystal structure determinations are listed in Table S1 of the Supporting Information. The crystals were selected under an inert atmosphere, covered with dry and degassed polyfluoroether oil and mounted on a nylon loop. Crystallographic data were collected using graphite monochromated Mo-Kα radiation (λ = 0.71073 Å) on a Bruker AXS-KAPPA APEX II diffractometer equipped with an Oxford Cryosystem open-flow nitrogen cryostat, at 150 K. Cell parameters were retrieved using Bruker SMART software [30] and refined using Bruker SAINT [31] on all observed reflections. Absorption corrections were applied using SADABS [32]. Structure solution and refinement were performed using direct methods with the programs SIR2014 [33] included in the package of programs WINGX-Version 2014.1 [34]. All hydrogen atoms were inserted in

idealized positions and allowed to refine riding on the parent carbon atom. All the structures refined to a perfect convergence. Graphic presentations were prepared with ORTEP-3 [35]. Data was deposited in CCDC under the deposit numbers 1815703 for **1a**, 1815704 for **1b**, 1815705 for **2a** and 1815706 for **2b**.

4.6. Solid state magnetic measurements

Magnetic properties were studied using a 6.5 T *S700X SQUID* (Cryogenic Ltd.) magnetometer. All the four samples were transferred to the sample holder in a glovebox. Due to its high air sensitivity, the sample **1b** was transferred to a quartz tube inside a glovebox, which was then sealed under dinitrogen. For all samples, the magnetic susceptibility was measured as a function of temperature in increasing temperature range 5–300 K using DC magnetic fields of 100 Oe or 500 Oe depending on the samples. The paramagnetic data was obtained after the correction for the core diamagnetism estimated using Pascal's constants, giving $\chi_D = -542\times10^{-6}$, $\chi_D = -589\times10^{-6}$, $\chi_D = -541\times10^{-6}$, and $\chi_D = -587\times10^{-6}$ emu mol^{-1}, for compounds **1a**, **1b**, **2a**, and **2b**, respectively.

4.7. Mössbauer spectroscopy

Mössbauer spectra of complexes **1a** and **1b** samples were collected between 295 and 1.7 K in transmission mode using a conventional constant-acceleration spectrometer and a 25 mCi ^{57}Co source in a Rh matrix. The velocity scale was calibrated using α-Fe foil. Isomer shifts, IS, are given relative to this standard at room temperature. The absorbers were obtained by gently packing the sample into a perspex holder inside a glovebox. Absorber thickness was calculated on the basis of the corresponding electronic mass-absorption coefficients for the 14.4 keV radiation, according to Long *et al*. (1983) [36]. Low-temperature measurements between 1.7 and 4 K were performed with the sample immersed in liquid He and above 4 K in He exchange gas. The spectra were fitted to Lorentzian lines using a non-linear least-squares method [37].

Acknowledgements

We thank Fundação para a Ciência e a Tecnologia, Portugal, for financial support (Projects UID/QUI/00100/2013 and UID/Multi/04349/2013) and for fellowships to T.F.C.C, C.A.F.

and P.T.G. (PD/BD/52372/2013–CATSUS PhD Programme, SFRH/BPD/112340/2015, and SFRH/BSAB/ 140115/2018, respectively).

References

[1] (a) T. J. J. Sciarone, C. A. Nijhuis, A. Meetsma, B. Hessen, Dalton Trans. (2006) 4896; (b) S. C. Bart, E. J. Hawrelak, E. Lobkovsky, P. J. Chirik, Organometallics 24 (2005) 5518.

[2] Y. Rechkemmer, F. D. Breitgoff, M. van der Meer, M. Atanasov, M. Hakl, M. Orlita, P. Neugebauer, F. Neese, B. Sarkar, J. van Slageren, Nat. Commun. 7 (2016) 10467.

[3] W. H. Harman, T. D. Harris, D. E. Freedman, H. Fong, A. Chang, J. D. Rinehart, A. Ozarowski, M. T. Sougrati, F. Grandjean, G. J. Long, J. R. Long, C. J. Chang, Dalton Trans. 2007 955.

[4] H. Hao, S. Bhandari, Y. Ding, Eur. J. Inorg. Chem. (2002) 1060.

[5] T. K. Panda, K. Yamamoto, K. Yamamoto, H. Kaneko, Y. Yang, H. Tsurugi, K. Mashima, Organometallics 31 (2012) 2268.

[6] D. M. Dawson, D. A. Walker, M. Thornton-Pett, M. Bochmann, J. Chem. Soc. Dalton Trans. (2000) 459.

[7] Y. Yoshida, S. Matsui, Y. Takagi, M. Mitani, T. Nakano, H. Tanaka, N. Kashiwa, T. Fujita, Organometallics 20 (2001) 4793.

[8] J.-S. Mu, Y.-X. Wang, B.-X. Li, Y.-S. Li, Dalton Trans. 40 (2011) 3490.

[9] V. C. Gibson, C. Newton, C. Redshaw, G. A. Solan, A. J. P. White, D. J. Williams, J. Chem. Soc. Dalton Trans. (2002) 4017.

[10] J. Li, H. Song, C. Cui, Appl. Organomet. Chem. 24 (2010) 82.

[11] C. S. B. Gomes, M. T. Duarte, P. T. Gomes, J. Organomet. Chem. 760 (2014) 167.

[12] R. M. Bellabarba, P. T. Gomes, S. I. Pascu, Dalton Trans. (2003) 4431.

[13] C. S. B. Gomes, P. T. Gomes, M. T. Duarte, R. E. Di Paolo, A. L. Maçanita, M. J. Calhorda, Inorg. Chem. 48 (2009) 11176.

[14] T. L. Poulos, Chem. Rev. 114 (2014) 3919.

[15] R. Banerjee, S. W. Ragsdale, Annu. Rev. Biochem. 72 (2003) 209.

[16] S. A. Carabineiro, L. C. Silva, P. T. Gomes, L. C. J. Pereira, L. F. Veiros, S. I. Pascu, M. T. Duarte, R. T. Henriques, Inorg. Chem. 46 (2007) 6880.

[17] S. A. Carabineiro, R. M. Bellabarba, P. T. Gomes, S. I. Pascu, L. F. Veiros, C. Freire, L. C. J. Pereira, R. T. Henriques, M. C. Oliveira, J. E. Warren, Inorg. Chem. 47 (2008) 8896.

[18] C. A. C. Figueira, P. S. Lopes, C. S. B. Gomes, L. F. Veiros, P. T. Gomes, CrystEngComm 17 (2015) 6406–6419.

[19] (a) S. D. Reid, A. J. Blake, C. Wilson, J. B. Love, Inorg. Chem. 45 (2006) 636;
(b) J. A. Wolny, M. F. Rudolf, Z. Ciunik, K. Gatner, S. Wolowiec, J. Chem. Soc. Dalton Trans. (1993) 1611;
(c) B. S. Manhas, B. C. Verma, S. B. Kalia, Polyhedron 14 (1995) 3549;
(d) B. S. Jaynes, L. H. Doerrer, S. Liu, S. J. Lippard, Inorg. Chem. 34 (1995) 5735.

[20] (a) F. A. Cotton, G. Wilkinson, C. A. Murillo, M. Bochmann, Advanced Inorganic Chemistry; 6th ed., Wiley, 1999, pp.784 and 821;
(b) N. N. Greenwood A. Earnshaw, Chemistry of the Elements, 2nd ed., Elsevier Butterworth-Heinemann, 1997, pp.1092 and 1132.

[21] L. Yang, D. R. Powell, R. P. Houser, Dalton Trans. (2007) 955.

[22] (a) Y.-Z. Liu, J. Wang, Y. Zhao, L. Chen, X.-T. Chen, Z.-L. Xue, Dalton Trans. 44 (2015) 908;
(b) E. J. Hawrelak, W. H. Bernskoetter, E. Lobkovsky, G. T. Yee, E. Bill, P. J. Chirik, Inorg. Chem. 44 (2005) 3103.
(c) P.-H. Lin, N. C. Smythe, S. I. Gorelsky, S. Maguire, N. J. Henson, I. Korobkov, B. L. Scott, J. C. Gordon, R. T. Baker, M. Murugesu, J. Am. Chem. Soc. 133 (2011) 15806.

[23] O. Kahn, Molecular Magnetism, VCH Publishers Inc., New York, 1993, ch. 2, pp. 9–29.

[24] S. K. Langley, N. F. Chilton, B. Moubaraki, K. S. Murray, Dalton Trans. 40 (2011) 12201.

[25] S. Gomez-Coca, E. Cremades, N. Aliaga-Alcalde, E. Ruiz, J. Am. Chem. Soc., 135 (2013) 7010.

[26] J. M. Zadrozny, J. R. Long, J. Am. Chem. Soc. 133 (2011) 20732.

[27] N. N. Greenwood, T. C. Gibb, Mössbauer Spectroscopy, Chapman and Hall, Ltd. Publishers, London, England, 1971.

[28] G. M. Bancroft, Mössbauer Spectroscopy: An Introduction for Inorganic Chemists and Geochemists, McGraw-Hill, London, 1973.

[29] (a) D. F. Evans, J. Chem. Soc. (1959) 2003;
(b) S. K. Sur, J. Magnet. Res. 82 (1989) 169.

[30] SMART Software for the CCD Detector System Version 5.625, Bruker AXS Inc., Madison, WI, USA, 2001.

[31] SAINT Software for the CCD Detector System, Version 7.03, Bruker AXS Inc., Madison, WI, USA, 2004.

[32] G. M. Sheldrick, SADABS, Program for Empirical Absorption Correction, University of Göttingen, Göttingen, 1996.

[33] M. C. Burla, R. Caliandro, B. Carrozzini, G. L. Cascarano, C. Cuocci, C. Giacovazzo, M. Mallamo, A. Mazzone, G. Polidori, J. Appl. Cryst. 48 (2015) 306.

[34] L. J. Farrugia, J. Appl. Crystallogr. 32 (1999) 837.

[35] M. N. Burnett, C. K. Johnson, ORTEP-III: Oak Ridge Thermal Ellipsoid Plot Program for Crystal Structure Illustration, Oak Ridge National Laboratory, 1996. Report ORNL-6895.

[36] G. J. Long, T. E. Cranshaw, G. Longworth, Mossb. Effect. Ref. Data J. 6 (1983) 42.

[37] J. C. Waerenborgh, D. P. Rojas, A. L. Shaula, G. C. Mather, M. V. Patrakeev, V. V. Kharton, J. R. Frade, Mater. Lett. 59 (2005) 1644.